AIMS Materials Science, 11(4): 666–683.
DOI: 10.3934/matersci.2024034
Received: 17 June 2024
Revised: 23 July 2024
Accepted: 29 July 2024
Published: 12 August 2024

https://www.aimspress.com/journal/Materials

Research article

The impact of technological parameters of electrolytic-plasma treatment on the changes in the mechano-tribological properties of steel 45

Bauyrzhan Rakhadilov[1], Rinat Kussainov[2,*], Aisulu Kalitova[3], Zarina Satbayeva[1] and Aibek Shynarbek[2]

[1] Plasma Science LLP, Ust-Kamenogorsk 070000, Kazakhstan
[2] Engineering Center "Strengthening Technologies and Coatings", Shakarim University of Semey, Semey 071412, Kazakhstan
[3] Institute for Composite Materials, Ust-Kamenogorsk 070000, Kazakhstan

* **Correspondence:** Email: rinat.k.kus@mail.ru; Tel.: +7-705-369-9848.

Abstract: This article presents the results of research on the effects of electrolyte plasma hardening on the structure, phase composition, tribological, and mechanical properties of medium-carbon structural steel 45, which is widely used in the manufacturing of tools and machine parts. Hardening experiments were conducted using an electrolyte plasma hardening setup with electrolytes varying in sodium carbonate (Na_2CO_3) concentration in distilled water (15%, 20%, and 25%). With a consistent heating duration of 4 s during quenching, significant phase changes in the steel's microstructure were observed, enhancing hardness and wear resistance. The transformation of the initial structure of steel 45, which consists of ferrite and pearlite into martensite on the surface of the samples, led to an increase in microhardness up to 506–690 HV_{01}. This value is 2.5–3.5 times higher compared to the untreated sample, and the thickness of the hardened layer reached up to 3.2 mm. Additionally, wear volume measurements showed that after electrolyte plasma hardening, the wear resistance of the samples increased by 1.3–1.5 times (2.01×10^{-4}, 2.26×10^{-4} m^3). The obtained results on the changes in microstructure and mechano-tribological properties of steel 45 confirm the potential of electrolyte plasma hardening technology for improving operational characteristics and extending the service life of heavily loaded and critical machine parts.

Keywords: electrolytic plasma hardening; microstructure; phase transformations; microhardness; martensite

1. Introduction

Steel 45, similar to its counterpart AISI 1045, is widely used in mechanical engineering due to its balanced combination of strength and ductility. In agricultural machinery, such as plows and cultivators, steel 45 is used for manufacturing working parts that are subjected to significant mechanical loads and abrasive wear [1–4]. It is known that the performance of machine parts largely depends on the condition of their surface layers, as this is where microcracks that lead to wear and damage typically develop [5–8]. Traditional steel heat treatment techniques, such as bulk quenching in water or oil to enhance mechanical properties, are associated with some drawbacks, including the risk of internal stresses, deformations, and cracks due to uneven cooling, especially in large and complex parts. Thus, more technologically advanced methods of surface hardening, such as highly concentrated energy flows quenching (HCEFQ), are often employed.

The high concentration of energy supplied and its localized application allow for the treatment of only the surface portion of the material without heating the entire volume or disrupting its structure and properties, leading to minimal warping. This facilitates rapid heating and cooling of the treated material volume in a very short period. Depending on the specific method of highly concentrated energy flows quenching, it is possible to control the quality of the surface layer's structure, such as its hardness, wear resistance, roughness, and the geometric dimensions of the treated areas [9–12]. Laser quenching and electron beam techniques achieve a very high energy density (100 J/cm^2) and a rapid heating rate up to 10^4 K/s. Thanks to these high rates of heating and cooling (over 1000 K/s), a fine martensitic structure is formed [13]. These hardening methods also allow for precise control over the treatment areas, reducing the risk of damage to adjacent sections and minimizing deformation and stress in the treated part.

Another widely used method of HCEFQ is plasma quenching, which employs a plasma arc from ionized gas generated at high temperatures to heat the treated surface [14,15]. The method of plasma surface hardening also provides the ability to achieve much higher rates of heating and cooling compared to traditional hardening methods, which aids in forming hardened layers [16,17]. Heating with a plasma arc can raise the surface temperature of the part to high levels (above AC3 point) and rapidly cool it by transferring heat to the inner layers of metal. This results in quenched structures with high hardness, wear resistance, and resistance to breakdown [18,19].

However, the widespread implementation of the above-mentioned hardening methods using concentrated energy flows in industry is hindered due to the high cost of equipment, its complexity, the need for specialized facilities and qualified maintenance, as well as significant operational expenses. In this context, electrolytic plasma processing (EPP) technology is a promising direction in steel treatment to extend the service life of rapidly wearing parts. Recent intensive research in this area highlights the following distinctive qualities of the EPP technology: versatility, accessibility, and environmental friendliness [20–23]. Additionally, unlike plasma quenching, EPP allows for surface polishing and a series of chemical-thermal steel treatments such as carburizing, nitriding, and boriding depending on technological parameters [24–27]. From a resource-saving perspective, the method of electrolytic plasma hardening (EPH) or quenching, characterized by rapid heating followed by rapid cooling in an electrolytic medium, is particularly relevant [28–31]. It is also noted that EPH results in a lesser degree of oxide layer formation. This method allows for a wide range of adjustments in heating and cooling rates, thereby modifying the structure and thickness of the hardened layer. Electrolytic plasma quenching is used to enhance wear resistance and extend the service life of critical components

in industries such as mechanical engineering, aerospace, and agriculture. This technology is also employed in the manufacturing of tools and equipment to achieve increased hardness and improved tribological surface properties.

In the process of electrolytic plasma hardening, flowing aqueous solutions of salts and other substances serve as the electrolyte and complete the electrical circuit, enabling the transformation of electrical energy into heat in the layer of electrolyte adjacent to the cathode. Heated by the energy, the electrolyte vaporizes, forming a vapor-gas shell around the cathode and causing an intense arc discharge, which leads to the formation of electrolytic plasma. The power released in this plasma can reach up to 3×10^3 W/cm^2 [32]. Such heating, followed by rapid cooling in the electrolyte, alters the microstructure of steels, affecting their mechanical and physical properties. A key factor influencing phase transformations during electrolytic plasma heating is the periodic increase in temperature, where the metal is heated above the $\alpha \rightarrow \gamma$ phase transition temperature. Subsequent rapid cooling transforms the austenite into structures such as martensite or bainite, preventing the formation of ferrite. The deeper heat affected zone (HAZ) includes a fine-grained structure typical of the hardened layer and a coarse-grained structure characteristic of the substrate.

Several studies have focused on the impact of electrical parameters in electrolytic plasma quenching on steel properties. One such study by L. Cenk Kumruoglu and Ahmet Özel examined the effects of electrolytic plasma cyclic treatment on AISI 4140 steel [33]. The experiment involved cyclically changing the voltage between 320 and 250 V using a 17.6% sodium carbonate (Na_2CO_3) aqueous solution as the electrolyte. The study also explored how different voltage levels and durations of electrolytic plasma quenching affected the mechanical properties and structural-phase states of AISI 4140 steel. The quenching process achieved a maximum hardness of 770 HV_{01}, and fine phases of martensite and pearlite were analyzed from the surface down to the core of the material. Under processing parameters of 300–320 V for 42 s, the maximum thickness of the treated layer reached approximately 10 mm, with a microhardness of 500–650 HV_{01}, which is 4 to 5 times higher than that of the base material.

Another study [34] investigated the surface hardening and microstructural modification of 40X steel following electrolytic plasma cyclic quenching. A 15% solution of Na_2CO_3 in distilled water was used as the electrolyte. The voltage and quenching time were cyclically changed, set at 320, 250, and 50 V. The researchers noted that the cyclic change in voltage allowed for the stabilization and delay of the heating rate. The microhardness was highest during a single quenching lasting 2 s, and the greatest thickness of the hardened layer was achieved over 7 cycles of voltage switching.

The electrolyte also plays a crucial role in the EPH process, serving as a cooling medium. Its ability to vary the cooling rate depending on the composition provides flexibility in choosing parameters, similar to traditional bulk quenching methods, including the heat treatment of steel 45. This approach effectively applies the experience accumulated in traditional bulk quenching to the processes of electrolytic plasma hardening. The choice of cooling medium significantly influences the thermodynamic parameters of the process, determining its efficiency and the final properties of the material [35]. For instance, a higher salt concentration speeds up the cooling process, which contributes to an increase in steel hardness [36–39]. In the study by Basori et al., the bulk quenching of AISI 1045 steel was conducted using a pure water and salt solution (NaCl) in various ratios as the cooling medium [40]. Austenitization was carried out at 850 °C in a muffle furnace with varying time intervals—15 and 30 min. Quenching the samples in salt solutions with different concentrations showed

that increasing the time and salt concentration enhances the formation of martensite and increases hardness, though it decreases the material's toughness.

Researchers, including E.A. Pérez R., conducted quenching of steel in various environments, including water and mixtures of water with machining fluid in different proportions [41]. When quenching in water, additional tempering was performed at 400 °C. Results showed a reduction in the friction coefficient and wear volume in all samples compared to untreated steel. Interestingly, using a mixture of 60% water and 40% machining fluid achieved the same levels of friction coefficient and wear volume as after tempering, suggesting the possibility of skipping this processing stage. However, using machining fluid at a lower concentration led to higher hardness levels, while higher concentrations resulted in reduced hardness.

In another study led by Eduardo da Rosa Vieira, it was emphasized that increasing the concentration of polymer solutions leads to the formation of coarse-grained martensite, which reduces hardness compared to samples cooled in less concentrated solutions [42]. This is due to the slowed heat removal, reducing the ability to form martensite and resulting in steel with lower hardness and strength.

Electrolytic plasma quenching, depending on the composition of the electrolyte, can achieve cooling rates up to 500 °C/s, whereas cooling rates between 150 and 200 °C/s are sufficient to transform austenite into martensite [35,43,44]. In EPH, the electrolyte not only functions as a cooling medium but also contributes to the creation of a vapor-gas shell, meaning the composition of the electrolyte can affect the properties of the quenched material through mechanisms different from those used in traditional quenching methods. In the study by M. R. Bayati, the impact of voltage, duration of EPH, and various electrolyte compositions on the surface microhardness of AISI 1045 steel was investigated [45]. The electrolyte used was an aqueous solution of chromium chloride ($CrCl_3 \cdot 6H_2O$) at concentrations of 5%, 10%, and 15%. After setting the processing mode, the current was switched on and off after a set time, and the sample was cooled in the electrolyte. The authors note that higher microhardness was observed for more concentrated electrolytes. As the specific resistance of the electrolyte, and thus the overall resistance of the electrochemical cell, decreases with increasing electrolyte concentration, the voltage applied to the surface of the cathode increases. Consequently, the cathode surface emits more heat, and austenitization is more complete.

In study [46], different electrolyte compositions containing Na_2CO_3 were selected to ensure optimal electrical conductivity and urea to prevent decarburization. It was noted that high hardness of samples made from alloy steel 40Kh is observed in electrolytic plasma quenching using electrolytes containing 15% and 20% urea and 10%–15% Na_2CO_3. The lowest hardness was shown by samples treated in electrolytes containing 10% urea and 15%–20% Na_2CO_3.

As mentioned above, the main mechanical and tribological qualities of steel improved during EPH, such as hardness, thickness of the modified layer, and wear resistance, depend on the current density, voltage, electrolyte temperature, processing time, and composition of the electrolyte. Among these factors, the composition of the electrolyte plays a crucial role, hence the study on the impact of electrolyte composition on the properties of steel 45 is very important.

The article aims to provide a comprehensive study of the impact of technological parameters of electrolytic plasma hardening, mainly the composition of the electrolyte, on the structural, phase, mechanical, and tribological characteristics of steel 45. This research is intended to deepen the understanding of the key mechanisms of this process, assess its effectiveness, and explore its application possibilities in various industrial sectors.

2. Materials and methods

EPH of steel grade 45 samples was carried out using an electrolytic plasma processing installation located at the Shakarim University of Semey, designed for the surface hardening of soil-cultivating machine components. The installation consists of a 50 kW direct current (DC) power source, an electrolyte bath, an electric pump, and a conical anode made of stainless steel, into which the electrolyte is fed. The scheme and external appearance of this installation are shown in Figure 1. The operation principle of the installation involves applying voltage between the anode and the cathode, which is the sample under test, while the electrolyte circulates between them, pumped from the electrolyte bath using the electric pump. The current flowing through the medium from the metallic cone anode to the liquid electrolyte and metallic cathode generates heat in the cathode-sample due to the Joule-Lenz law. The liquid electrolyte, upon reaching boiling temperature, vaporizes, thus creating a vapor-gas shell around the cathode due to localized boiling. Further heating to a certain temperature and critical voltage value creates electrolytic plasma. Thus, the cathode-sample is heated to quenching temperature, and when the power is turned off, it cools in the electrolyte environment [32,44,47]. The DC power source provides the necessary voltage levels at the cathode according to a pre-set program, allowing EPH to be performed in various modes, including cyclic quenching.

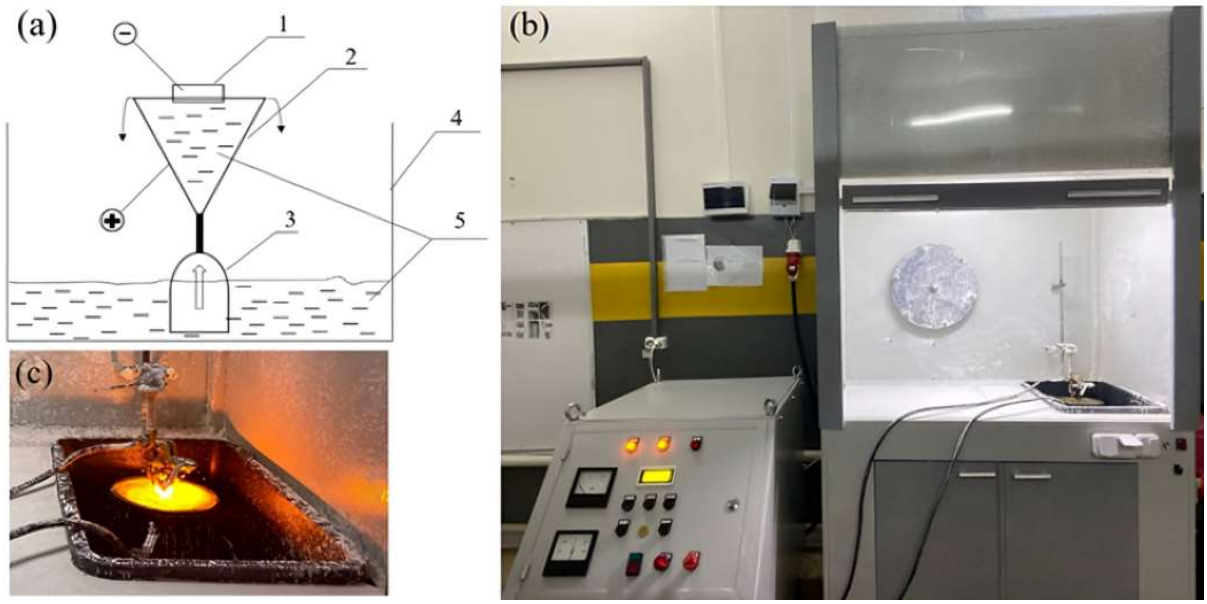

Figure 1. Functional schematic of the electrolytic plasma surface hardening installation: (a) 1: sample being processed (cathode), 2: stainless steel anode in the shape of a cone, 3: pump, 4: working chamber-bath with electrolyte, 5: electrolyte; (b) external view of the electrolytic plasma surface hardening installation; and (c) the quenching process.

The samples for the experiment were cut from a 65 mm diameter rod of steel grade 45 according to GOST 7417-75, all of the same size: 15 × 15 × 15 mm. The chemical composition of steel 45 is shown in Figure 2. The surfaces of the samples were leveled on a TROJAN GP-1A grinding machine and then manually processed on a flat glass covered with abrasive paper. During the grinding process, the samples were transitioned from coarse to finer grit sizes, ranging from P100 to P2500. Any

remaining scratches from the final sanding were removed by polishing on a loose cloth using a special paste containing suspensions of dispersed chromium oxide particles.

C	0.42-0.50
Si	0.17-0.37
Mn	0.50-0.80
Ni	>0.25
S	>0.04
P	>0.035
Cr	>0.25
Cu	>0.25
As	>0.08
Fe	~97

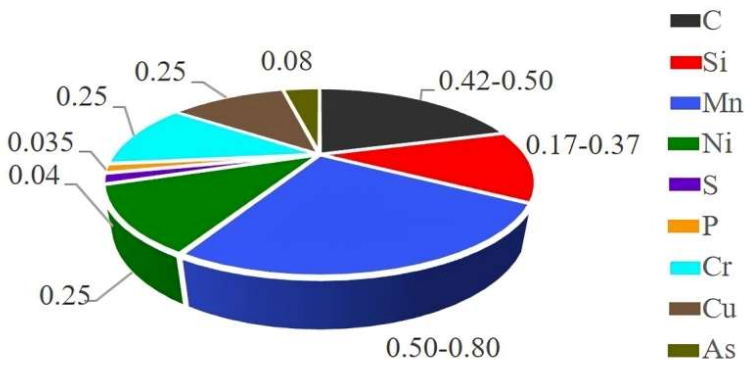

Figure 2. Chemical composition of steel 45 (excluding iron, elements listed in the diagram).

In the experiments, different compositions of the electrolyte containing Na_2CO_3 and distilled water were used, while the supplied voltage (U, V), duration of treatment (t, s), and the flow rate of the electrolyte for all samples were kept constant. The parameters of electrolytic plasma hardening are presented in Table 1.

Table 1. Parameters of EPH regimes for steel 45.

Sample	Electrolyte composition	Electrolyte flow rate (L/min)	Voltage (V)	Anode area (cm^3)	Anode-cathode distance (cm)	Current density (A/cm^2)	Time (s)
No. 1	15% Na_2CO_3 + 85% water	100	300	500	10	36	4
No. 2	20% Na_2CO_3 + 80% water	100	300	500	10	44	4
No. 3	25% Na_2CO_3 + 75% water	100	300	500	10	44	4

The experimental studies were conducted at the Scientific Research Center "Surface Engineering and Tribology" (S. Amanzholov East Kazakhstan University, Oskemen, Kazakhstan) and at the Engineering Center "Strengthening Technologies and Coatings" (Shakarim University of Semey, Semey, Kazakhstan). The phase composition of the samples was investigated using an X'PertPro X-ray diffractometer (Philips, Netherlands) with Cu-Kα radiation. Data processing and quantitative analysis were performed using X'Pert HighScore Plus software (version: 3.0, reference code: 00-044-1290). Sample preparation, visualization modes selection, and diffractogram calculations were conducted according to the methodologies described in [48].

For optical microscopy of the samples structure, an Altami 5C metallographic microscope (Russia) was used. A TESCAN VEGA S5122 scanning electron microscope was also employed for studying

the microstructure at magnifications of ×4000 and ×10000. Before examining the microstructure, the samples underwent polishing and etching with a 4% solution of HNO_3 in ethyl alcohol.

The measurement of microhardness of the samples in their initial state and hardened steel was performed using a Vickers microhardness tester HV-1 DT, with loads on the indenter P = 1 N and a dwell time of 10 s (GOST 9450-76). The final value was the average of ten measurement results for all samples.

Tribological tests were conducted on an Anton Paar TRB3 tribometer using the ball-on-disk scheme under the following regime: wear radius—3 mm, friction path—60 m, rotation speed of the sample—2 cm/s, load 6 N. A 100Cr6 steel ball with a diameter of 6 mm was used as the counterbody. To measure the volume of wear, a HY2300 precision roughness tester was used.

3. Results and discussion

The microstructure of steel 45 before electrolytic plasma hardening is shown in Figure 3. From the microphotograph, it is evident that the original structure of steel 45 consists of a mix of ferrite (F—light areas) and pearlite (P—dark areas). Ferrite, being a soft and ductile phase, is distributed as light fields, while pearlite, consisting of alternating layers of ferrite and cementite, forms the darker sections of the structure [4,34,49].

After performing cathodic EPH on samples in electrolytes containing 15%, 20%, and 25% Na_2CO_3, as seen in Figure 3b–d, the steel surface structure undergoes significant changes.

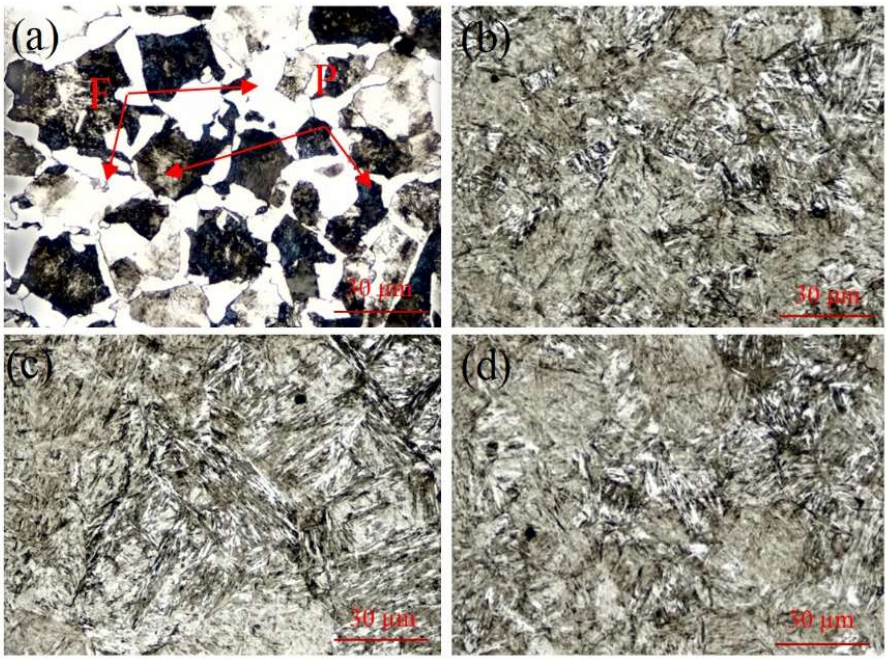

Figure 3. The surface morphology of steel 45 samples before and after EPH using various electrolyte solutions (×50): (a) initial; (b) 15% Na_2CO_3, 85% distilled water (sample No. 1); (c) 20% Na_2CO_3, 80% distilled water (sample No. 2); (d) 25% Na_2CO_3, 75% distilled water (sample No. 3).

Rapid heating for 4 s followed by swift cooling results in the formation of acicular martensite structures. As mentioned earlier, the cooling rate in these electrolytes is sufficient to reach the critical cooling rate necessary for the martensitic transformation of austenite. As shown in Figure 3, the intensity of the martensitic phases does not vary significantly among the samples after EPH.

Figure 4 presents the results of X-ray diffraction analysis obtained from the surfaces of the steel 45 samples. The diffractograms show the main peaks corresponding to alpha-iron at angles 2θ = 44.4°, 64.7°, and 82.1°, with Miller indices (110), (200), and (211), respectively [50,51]. After quenching, the peaks of alpha-iron in the diffractograms become less intense and broader, indicating the formation of martensite due to rapid cooling. Such changes in the diffraction pattern confirm phase transformations and an increase in internal stresses within the steel structure. These stresses arise due to distortions in the crystal lattice caused by the dissolution of carbon during quenching.

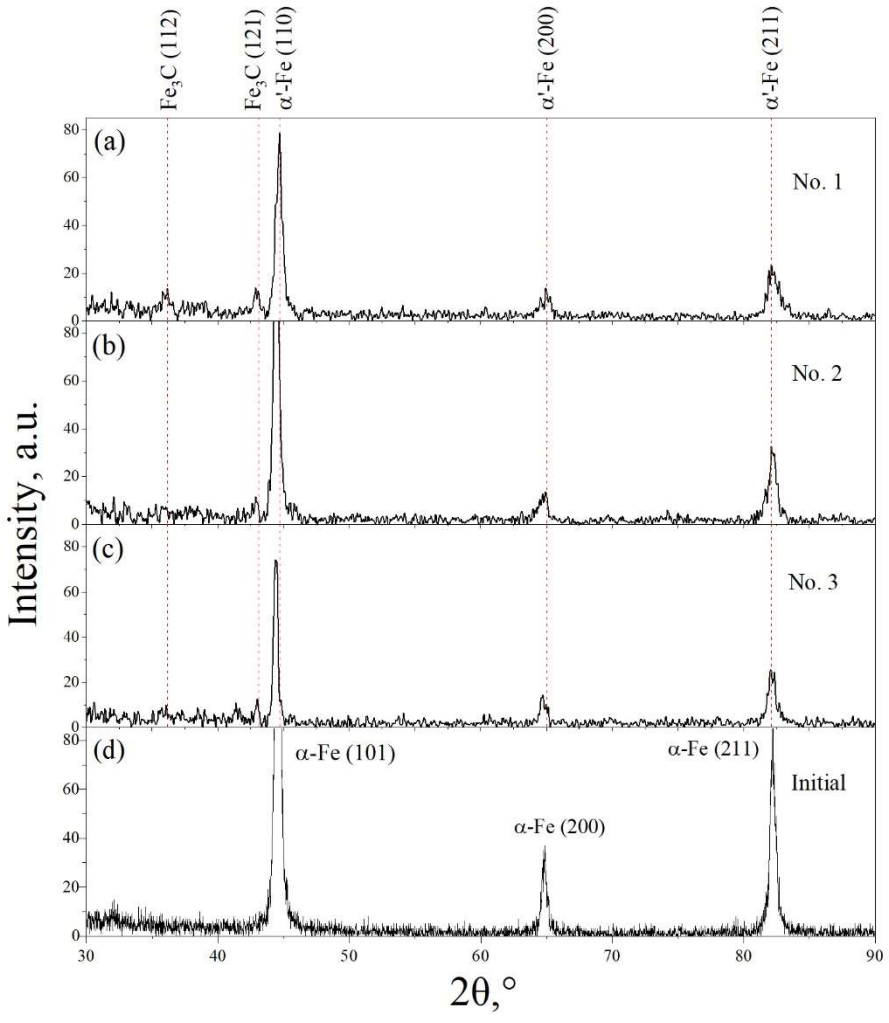

Figure 4. X-ray diffraction patterns on the surface of AISI 1045 steel specimens before and after EPH processing: (a) No. 1, (b) No. 2, (c) No. 3, (d) initial.

The results of the X-ray structural analysis are consistent with the quenching processes based on the iron-carbon phase diagram. These findings confirm significant changes in the phase composition of the steel's microstructure, which impact its mechanical properties and enhance its wear resistance.

Also visible in the figure is a small amount of cementite Fe_3C present after quenching. According to studies published in works [52–54], cementite forms on the steel surface after electrolytic plasma processing in an electrolyte containing Na_2CO_3. Interestingly, a Rietveld quantitative analysis showed an increase in the proportion of cementite with increasing Na_2CO_3 concentration in the electrolyte by 0.5%, 1.5%, and 2.5%, respectively, for samples No. 1, No. 2, and No. 3.

Figure 5 displays the microhardness values of the samples, measured using the Vickers method on their surface. After EPH, the hardness of samples No. 1 and No. 2 are not significantly different, at 690 HV_{01} and 675 HV_{01}, respectively, while sample No. 3 is considerably lower at 565 HV_{01}. The change in microhardness is due to the formation of martensitic structures in the steel, indicating a significant increase compared to the original sample (209 HV_{01}), whose microstructure consists of softer and more ductile ferrite and pearlite phases [32,55,56].

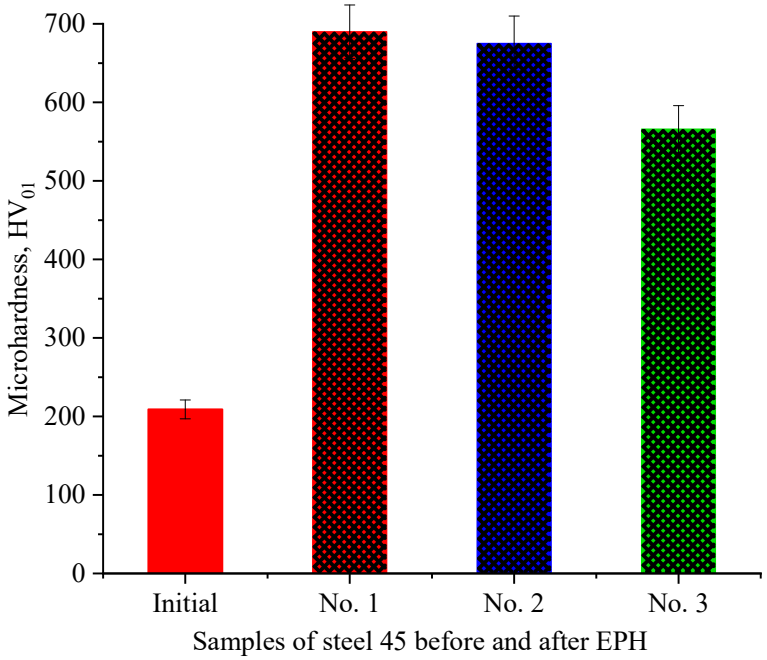

Figure 5. Surface microhardness measurements of steel 45 samples before and after 4 s of EPH using various electrolyte solutions: initial; 15% Na_2CO_3, 85% distilled water (sample No. 1); 20% Na_2CO_3, 80% distilled water (sample No. 2); 25% Na_2CO_3, 75% distilled water (sample No. 3).

Figure 6 shows the results of tribological tests on the surfaces of steel 45 samples using the "ball-disc" scheme, which includes measurements of the friction coefficient (Figure 6a) and wear volume (Figure 6b). From Figure 6a, it can be seen that the friction coefficient after EPH does not differ significantly from the original sample, with the lowest value corresponding to sample No. 1.

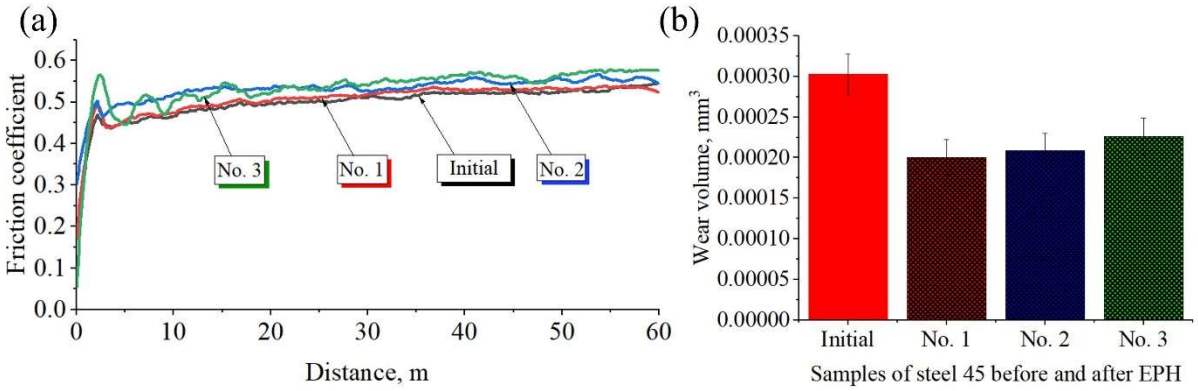

Figure 6. (a) Friction coefficient values and (b) wear volume of steel 45 samples before and after 4 s of EPH using various electrolyte solutions: initial; 15% Na_2CO_3, 85% distilled water (sample No. 1); 20% Na_2CO_3, 80% distilled water (sample No. 2); 25% Na_2CO_3, 75% distilled water (sample No. 3).

The study of wear resistance of steel 45 samples before and after EPH showed that the treated samples demonstrate a reduced wear volume compared to the originals (Figure 6b). This indicates an increase in wear resistance after EPH. Samples No. 1 and No. 2 showed the best results, with a reduction in wear volume by 33% compared to the original sample, while sample No. 3 showed a 25% improvement in wear resistance.

The study of microhardness and wear resistance of the steel 45 surface after EPH demonstrated a correlation between these parameters. The best results were achieved using electrolytes containing 15% and 20% Na_2CO_3. Although theoretically, an increase in concentration to 25% was expected to lead to greater heating and cooling rates, the expected level of increase in microhardness and wear resistance did not occur. Nevertheless, EPH generally had a positive effect on the mechano-tribological properties of all steel 45 samples.

It should also be noted that the obtained microhardness values are comparable to those achieved through traditional quenching or other methods using concentrated energy flows [8,22]. For example, in bulk quenching, the hardness of AISI 1045 steel reaches 650 HV [57], while electron beam irradiation results in a hardness of 726 HV [50]. In studies involving laser carbonitriding and plasma quenching, the wear volume was reduced by up to 80% [58,59]. However, in experiments with bulk quenching of AISI 1045 steel, the wear volume remained at pre-quench levels [41]. It is important to note that different wear volume measurement methods and various counterbody materials were used in these studies, which complicates direct comparison of these parameters. Nevertheless, a reduction in wear volume by up to 33% in electrolytic plasma quenching using an electrolyte containing 15% and 20% Na_2CO_3 indicates a significant increase in wear resistance and the effectiveness of this technology.

Figures 7 and 8 present microstructural changes in steel 45 after electrolytic plasma hardening, detailing the complex phase transformations throughout the depth of the sample. In the base metal (Figures 7f and 8f), a typical dispersion of ferrite and pearlite characteristic of untreated steel with a carbon content of about 0.45% is observed.

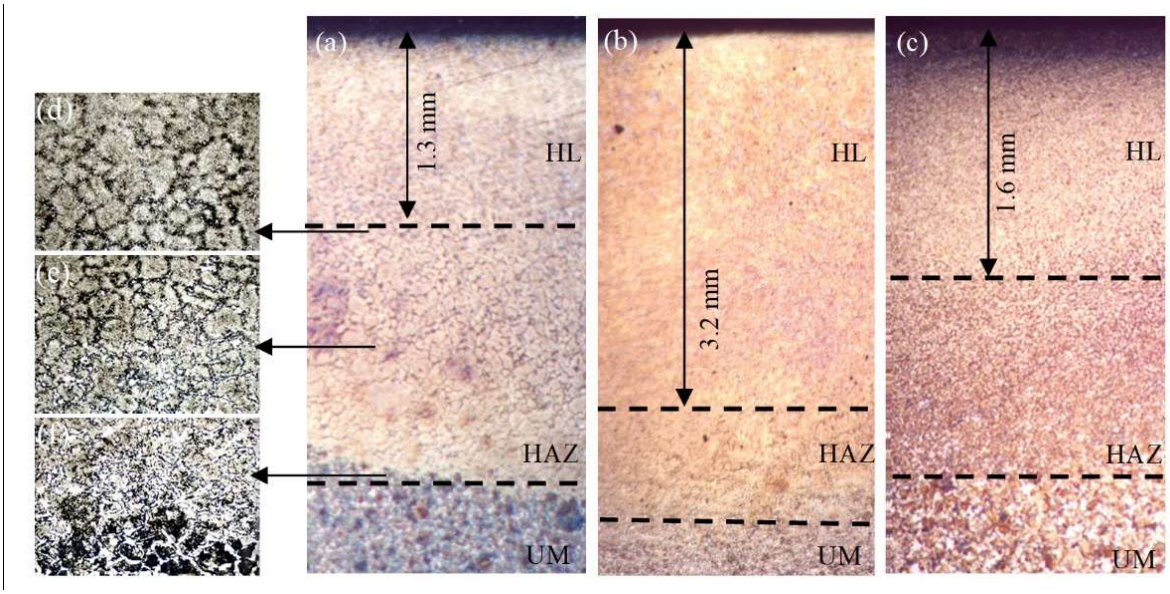

Figure 7. Microphotographs of the cross-section of steel 45 samples: (a) sample No. 1, (b) sample No. 2, (c) sample No. 3, HL—hardened layer, HAZ—heat affected zone, UM—unaffected material (×2), (d,e,f) the transition zones from the hardened layer to the base metal (×20).

In the heat affected zone (Figure 7e and 8e), which undergoes direct thermal impact, the metal transitions from fine-grained bainite to more finely dispersed pearlite, providing a balance between ductility and strength. The HAZ serves as a transitional area between the base metal and the hardened layer, providing gradient changes in microstructure. In this zone, a gradual transition occurs from pearlite and ferrite of the main matrix to the more hardened structures of bainite and martensite, ensuring not only high surface hardness but also sufficient resistance to cracking in deeper layers. The most critical hardening zone undergoes stages of overheating to temperatures above the AC3 point, leading to the complete austenitization of the material and subsequent formation of martensite upon rapid cooling (Figure 8b). This creates a highly hardened acicular martensite structure, which significantly improves mechanical properties such as hardness and wear resistance [60].

Rapid cooling, initiated by the electrolyte environment, is crucial for achieving the desired structural transformations according to the iron-carbon phase diagram. The creation of such a microstructure not only enhances the physical properties of steel but also significantly improves its operational qualities, making steel 45 ideally suited for use in conditions that require high resistance to mechanical loads and wear.

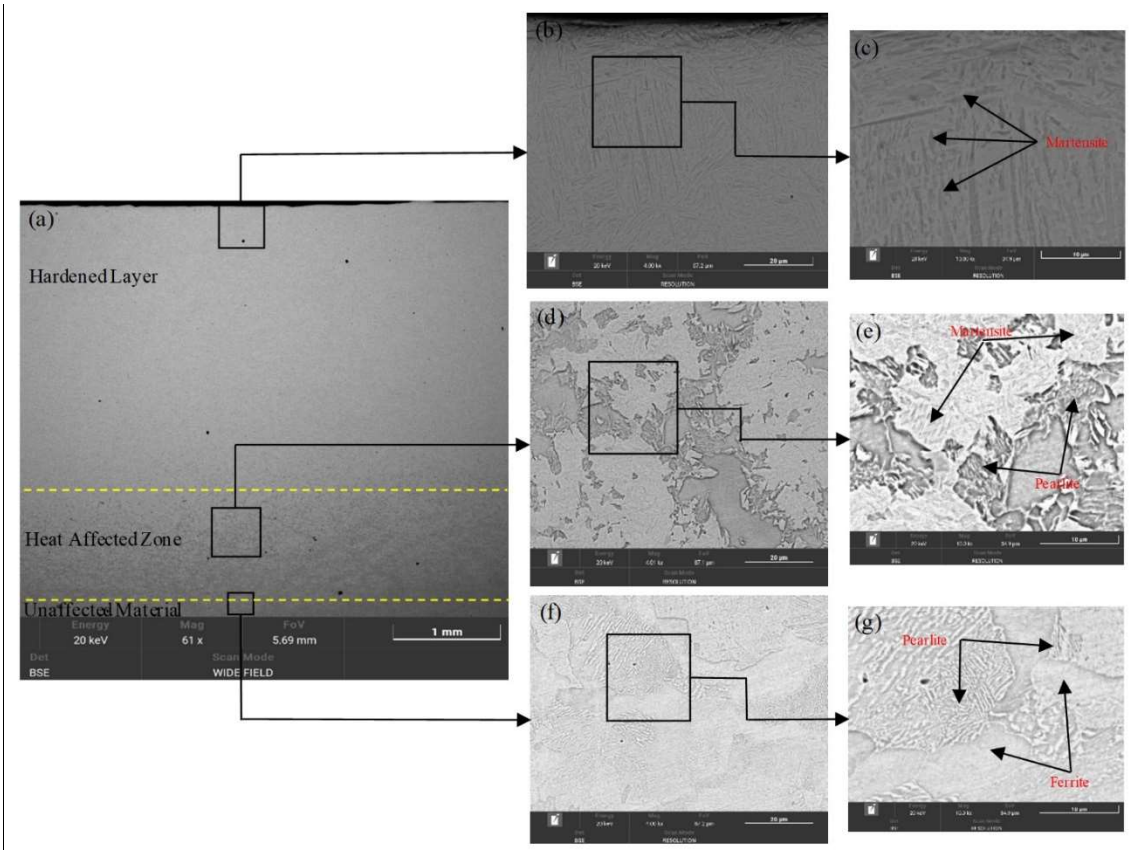

Figure 8. SEM images indicating the microstructure of sample No. 2 in cross-section: microphotography at (a) ×60, hardened layer at (b) ×4000 and (c) ×10000, heat affected zone at (d) ×4000 and (e) ×10000, original material at (f) ×4000 and (g) ×10000.

From the data in Table 2, it is apparent that the greatest thickness of the hardened layer of steel after electrolytic plasma processing with an electrolyte containing 20% Na_2CO_3 is 3.2 mm. Meanwhile, samples treated with electrolytes containing 15% and 30% Na_2CO_3 showed layer thicknesses of 1.3 and 1.6 mm, respectively. It was also noted that samples No. 2 and No. 3 have a relatively greater thickness of the hardened layer compared to the HAZ, unlike sample No. 1.

Table 2. Thickness of the hardened layer.

Sample	Hardened layer thickness (mm)
No. 1	1.30
No. 2	3.20
No. 3	1.60

Figure 9 presents data on the microhardness of sample No. 2 through the depth of the steel. The hardened layer exhibits hardness in the range of 600–675 HV_{01}, indicating the formation of a martensitic structure. In the heat affected zone, at a depth of 3.2–4.3 mm where bainite and high-dispersion pearlite predominate, the microhardness decreases from 600 HV_{01} to 200 HV_{01}. Beyond this depth, the microhardness stabilizes at 200 HV_{01}, corresponding to the original structure of steel 45.

Such a distribution of phases and structures in the heat affected zone after quenching creates unique transitional properties of the metal, where each layer possesses its specific microstructure and mechanical characteristics, optimizing them for different operating conditions. This makes steel 45 after electrolytic plasma hardening ideally suited for use in conditions of high loads and intense wear, such as in parts of machines and mechanisms. The distribution of phases and structures in this zone is critically important for achieving optimal hardness, strength, and wear resistance of the steel.

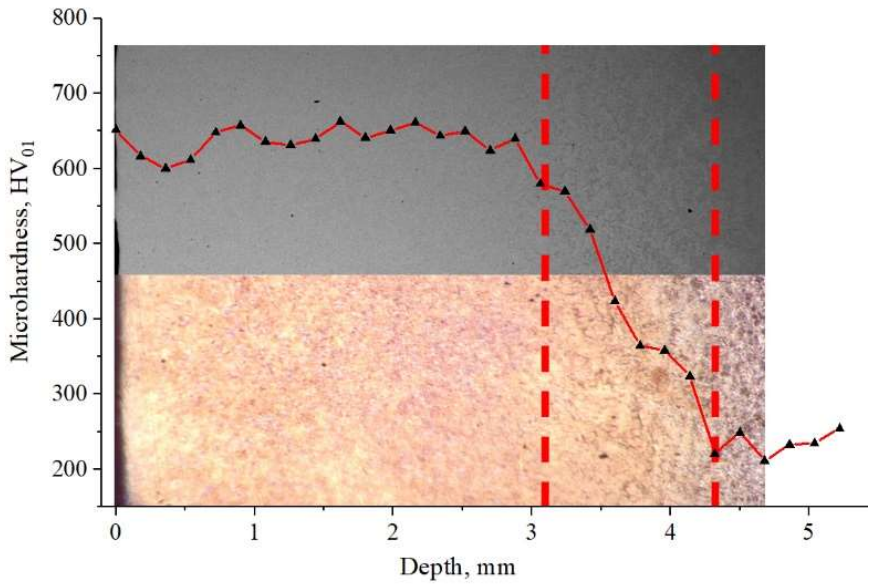

Figure 9. The distribution of hardness through the depth of steel 45 sample after EPH with an electrolyte containing 20% Na_2CO_3.

4. Conclusions

Electrolytic plasma hardening significantly impacted the microstructural and mechanical properties of steel 45, markedly enhancing its microhardness and wear resistance. The EPH facilitated the formation of a martensitic structure, which is harder and more wear-resistant compared to the original ferritic-pearlitic structure of the steel. X-ray diffraction analysis confirmed phase transformations in the steel after quenching and showed an increase in internal stresses within the material structure. Such changes contribute to the improvement of mechanical properties, especially hardness and resistance to mechanical loads.

The use of solutions with varying Na_2CO_3 content allowed for an increase in steel microhardness up to 690 HV_{01}, which is significantly higher than the initial sample (an increase of 3.5 times). Tribological tests showed a substantial reduction in the wear volume of the treated samples to 0.21×10^{-3} m^3, which is 1.5 times less than the untreated sample. The most optimal results were achieved using an electrolyte with a 20% Na_2CO_3 content, providing the best combination of microhardness, wear resistance, and depth of the hardened layer. It was also noted that different concentrations of Na_2CO_3 in the electrolyte during electrolytic plasma hardening have diverse effects on the properties of the steel. Specifically, samples treated with a 25% concentration of Na_2CO_3 exhibited lower hardness and wear resistance compared to samples treated at lower concentrations. However, the depth of the hardened layer was thicker compared to the sample treated with 15%

Na_2CO_3 content, indicating a complex balance between the depth of hardening and the achieved surface hardness.

Overall, the studies confirmed the effectiveness of using electrolytic plasma hardening technology for surface hardening of steel 45, which is actively used in the production of heavily loaded parts. This opens new perspectives for improving the operational properties of parts in automotive and agricultural machinery, providing increased resistance to mechanical and abrasive loads, enhancing wear resistance, and extending service life. The application of EPH allows for the expanded use of steel 45 by improving its key characteristics, which in turn contributes to the enhancement of overall production process efficiency and reduction in maintenance and repair costs. These advantages make EPH a valuable tool for improving the quality and durability of metal products across various industrial sectors.

Use of AI tools declaration

The authors declare they have not used Artificial Intelligence (AI) tools in the creation of this article.

Author contributions

Bauyrzhan Rakhadilov conceived the initial idea; Rinat Kussainov and Aibek Shynarbek conducted the experiment; Rinat Kussainov wrote the manuscript with the support of Aisulu Kalitova, and Aibek Shynarbek prepared the sample from steel 45; Zarina Satbayeva helped oversee the project; Aisulu Kalitova led the research. All authors discussed the results and contributed to the final manuscript.

Funding

This research has been funded by the Science Committee of the Ministry of Science and Higher Education of the Republic of Kazakhstan (Grant No. AP13068365).

Conflict of interest

The authors declare no conflict of interest.

References

1. Sharaya O, Vodolazskaya N (2019) Technological aspects of modification of surface layer of agricultural machines parts. *Inn Agric Compl Probl Perspect* 3: 82–92 (in Russian). Available from: https://www.bsaa.edu.ru/InfResource/library/Journal3(23)2019.pdf.
2. Aulov V, Rozhkov Y (2016) On the issue of combining electrospark and thermodiffusion methods for hardening the machine parts surfaces in the agribusiness. *Mach Equip Rural Area* 2: 28–32 (in Russian). Available from: https://doi.org/10.33267/2072-9642-2022-2-28-32.
3. Zobnev V, Markov A, Ivanov S, et al. (2014) Wear resistance of multicomponent diffusion boride coatings on working organs of agricultural machines. *Mater Sci Mach Build* 1: 435–439 (in Russian). Available from: https://elibrary.ru/download/elibrary_22610860_80996072.pdf.

4. Martínez-Vázquez J, Rodríguez-Ortiz G, Hortelano-Capetillo J, et al. (2021) Effect of induction heating on Vickers and Knoop hardness of 1045 steel heat treated. *J Mech Eng* 5: 8–15. https://doi.org/10.35429/JME.2021.15.5.8.15
5. Dudnikov I (2011) Ensure the safety properties of parts that define security of agricultural machinery. *Tech Audit Prod Res* 1: 33–36 (in Russian). https://doi.org/10.15587/2312-8372.2011.4853
6. Morshed-Behbahani K, Farhat Z, Nasiri A (2024) Effect of surface nanocrystallization on wear behavior of steels: A review. *Materials* 17: 1618. https://doi.org/10.3390/ma17071618
7. Pour-Ali S, Kiani-Rashid A, Babakhani A, et al. (2018) Severe shot peening of AISI 321 with 1000% and 1300% coverages: A comparative study on the surface nanocrystallization, phase transformation, sub-surface microcracks, and microhardness. *Int J Mater Res* 109: 451–459. https://doi.org/10.3139/146.111622
8. Roy R, Ghosh S, Kaisar T, et al. (2022) Multi-response optimization of surface grinding process parameters of AISI 4140 alloy steel using response surface methodology and desirability function under dry and wet conditions. *Coatings* 12: 104. https://doi.org/10.3390/coatings12010104
9. Stepanova T (2009) *Technologies of Surface Hardening of Machine Parts*, Ivanovo: Ivanovo State Chemical-Technological University, 64p (in Russian). Available from: https://www.isuct.ru/sites/default/files/department/ightu/ktmio/08.pdf.
10. Ostromenskiy P, Aksenov V, Korotaev B, et al. (2001) Prospects for the use of high-energy technologies to increase the lateral wear resistance of rails. *Curr Probl Transp Asian Part Russ* 2001: 92–98 (in Russian). Available from: https://is.gd/dUCNDS.
11. Maisuradze M (2022) *Induction and Laser Thermal Treatment of Steel Products: A Textbook*, Yekaterinburg: Ural University Publishing, 96p (in Russian). Available from: https://elar.urfu.ru/bitstream/10995/117127/1/978-5-7996-3544-2_2022.pdf.
12. Khisamutdinov R, Zvezdin V, Israfilov I, et al. (2016) Study of processes of steels surfaces modification with highly concentrated energy flows. *J Phys Conf Ser* 669: 012024. https://doi.org/10.1088/1742-6596/669/1/012024
13. Barmin A, Rizakhanov R, Rudstein R (2012) Optimization of quenching regimes for carbon steels by electron beam treatment. *Proc Interuniv Sci Sch Young Spec* 1: 62–67 (in Russian). Available from: http://nuclphys.sinp.msu.ru/school/s12/12_15.pdf.
14. Belinin D, Shchitsyn Y (2012) Features of structurization at plasma surface hardening on big depth of products from 40Cr13. *Proc Samara Sci Cent Russ Acad Sci* 4: 1200–1205 (in Russian). Available from: https://elar.urfu.ru/bitstream/10995/30926/1/sid_2014_04.pdf.
15. Belinin D, Verkhorubov V, Kuchev P, et al. (2011) Plasma surface hardening of hard loading constructions made of steel 40Kh13. *Bulletin Pnrpu* 2: 12–18 (in Russian). Available from: https://cyberleninka.ru/article/n/plazmennaya-zakalka-tyazhelonagruzhennyh-detaley-iz-stali-40h13.
16. Sidorov S (1998) Technical level and resource of working organs of agricultural machinery. *Tract Agric Mach* 3: 29 (in Russian). Available from: https://rusneb.ru/catalog/000200_000018_RU_NLR_PER_B_2381825_1998_3/.
17. Kravchenko N (2013) *Plasma Methods of Hardening and Restoration of Working Bodies Road-Building and Soil-Cultivating Machines*, Moscow: Eco-Press, 328 p (in Russian). Available from: https://expo-books.ru/category/book?id=12005.

18. Kanayev A (2015) Modernization of the surface layer structure of structural steel. *Herald Scin Seifullin Kaz Agro Tehn Univ* 3: 78–86 (in Russian). Available from: https://bulletinofscience.kazatu.edu.kz/index.php/bulletinofscience/article/view/701.
19. Korotkov V (2011) Wear resistance of plasma-hardened materials. *J Frict Wear* 32: 17–22. https://doi.org/10.3103/S1068366611010077
20. Jumbad V, Chel A, Verma U (2020) Application of electrolytic plasma process in surface improvement of metals: A review. *Letters Appl NanoBioSci* 9: 1249–1262. https://doi.org/10.33263/lianbs93.12491262
21. Gupta P, Tenhundfeld G, Daigle E (2007) Electrolytic plasma technology: Science and engineering—An overview. *Surf Coat Tech* 201: 8746–8760. https://doi.org/10.1016/j.surfcoat.2006.11.023
22. Rakhadilov B, Bayatanova L, Kurbanbekov S, et al. (2023) Investigation on the effect of technological parameters of electrolyte-plasma cementation method on phase structure and mechanical properties of structural steel 20X. *AIMS Mater Sci* 10: 934–947. https://doi.org/10.3934/matersci.2023050
23. Meletis E, Nie X, Wang F (2002) Electrolytic plasma processing for cleaning and metal-coating of steel surfaces. *Surf Coat Tech* 150: 246–256. https://doi.org/10.1016/S0257-8972(01)01521-3
24. Belkin P (2013) Electrolytic-plasma modification of metals and alloys. *Bull Kostroma State Univ* 5: 5–11 (in Russian). Available from: https://cyberleninka.ru/article/n/elektrolitno-plazmennaya-modifikatsiya-metallov-i-splavov-1.
25. Jiang Y, Bao Y, Wang M (2017) Kinetic analysis of additive on plasma electrolytic boriding. *Coatings* 7: 61. https://doi.org/10.3390/coatings7050061
26. Belkin V, Belkin P, Krit B, et al. (2019) Increasing wear resistance of low-carbon steel by anodic plasma-electrolytic nitroboriding. *J Mater Eng Perform* 29: 564–572. https://doi.org/10.1007/s11665-019-04521-1
27. Taheri P, Dehghanian C, Aliofkhazraei M, et al. (2007) Nanocrystalline structure produced by complex surface treatments: plasma electrolytic nitrocarburizing, boronitriding, borocarburizing, and borocarbonitriding. *Plasma Process Polym* 4: 721–727. https://doi.org/10.1002/ppap.200731805
28. Skakov M, Rakhadilov B, Sheffler M (2013) Influence of electrolyte plasma treatment on structure, phase composition and microhardness of steel P6M5. *Key Eng Mater* 531–532: 627–631. https://doi.org/10.4028/www.scientific.net/KEM.531-532.627
29. Luk S, Leung T, Miu W (1999) A study of the effect of average preset voltage on effective case depth during electrolytic surface-hardening. *Mater Charact* 42: 65–71. https://doi.org/10.1016/S1044-5803(98)00044-8
30. Tarakci M, Korkmaz K, Gencer Y (2005) Plasma electrolytic surface carburizing and hardening of pure iron. *Surf Coat Tech* 199: 205–212. https://doi.org/10.1016/j.surfcoat.2005.02.117
31. Satbayeva Z (2022) *Structure Formation in Alloyed Steels During Electrolytic-Plasma Surface Hardening*, Oskemen: Sarsen Amanzholov East Kazakhstan University, 160p (in Russian). Available from: https://nabrk.kz/ru/e-catalog?catalog=4&language=rus&page=8&sphere=3&topic=0&publication_type=13.
32. Suminov I (2011) *Plasma Electrolytic Modification of the Surface of Metals and Alloys*, Moscow: Tekhnosfera, 464 p (in Russian). Available from: https://f.eruditor.link/file/2686301/.

33. Cenk Kumruoğlu L, Özel A (2010) Surface modification of AISI 4140 steel using electrolytic plasma thermocyclic treatment. *Mater Manuf Process* 25: 923–931. https://doi.org/10.1080/10426911003720839
34. Sagdoldina Z, Zhurerova L, Tyurin Y, et al. (2022) Modification of the surface of 40Kh steel by electrolytic plasma hardening. *Metals* 12: 2071. https://doi.org/10.3390/met12122071
35. Smirnov M (1999) *Fundamentals of Heat Treatment of Steel*, Yekaterinburg: Ural Branch of the Russian Academy of Sciences, 494p (in Russian). Available from: http://www.materialscience.ru/ shared_folder/matved/books/Smirnov_Osnovy_TO_stali.djvu.
36. Kartonova L (2020) *Theory and Technology of Heat Treatment*, Vladimir: Publishing house of Vladimir State University, 128p (in Russian). Available from: https://dspace. www1.vlsu.ru/bitstream/123456789/8725/1/02082.pdf.
37. Rasouli D, Khameneh Asl S, Akbarzadeh A, et al. (2008) Effect of cooling rate on the microstructure and mechanical properties of microalloyed forging steel. *J Mater Process Technol* 206: 92–98. https://doi.org/10.1016/j.jmatprotec.2007.12.006
38. Sunardi S, Lusiani R, Listijorini E, et al. (2021) The effect of airflow speed as cooling media in the hardening process to the hardness, corrosion rate and fatigue life of medium carbon steel. *Mater Sci Forum* 1045: 40–49. https://doi.org/10.4028/www.scientific.net/msf.1045.40
39. Jo H, Kang M, Park G, et al. (2020) Effects of cooling rate during quenching and tempering conditions on microstructures and mechanical properties of carbon steel flange. *Materials* 13: 4186. https://doi.org/10.3390/ma13184186
40. Basori I, Pratiwi W, Dwiyati S (2019) Effect of salt quenching on the microstructures and mechanical properties of AISI 1045 steel. *J Phys Conf Ser* 5: 055102. https://doi.org/10.1088/1742-6596/1402/5/055102
41. Pérez R, Llano M, Ravagli R, et al. (2018) Effect of machining fluid like quenching media on the friction and wear behavior of AISI 1045 steel. *Int J Mech Eng Technol* 9: 146–154. Available from: https://iaeme.com/MasterAdmin/Journal_uploads/IJMET/VOLUME_9_ISSUE_7/IJMET_09_07_017.pdf.
42. Vieira E, Biehl L, Medeiros J, et al. (2021) Evaluation of the characteristics of an AISI 1045 steel quenched in different concentration of polymer solutions of polyvinylpyrrolidone. *Sci Rep* 11: 1313. https://doi.org/10.1038/s41598-020-79060-0
43. Dayanç A, Karaca B, Kumruoğlu L (2017) The cathodic electrolytic plasma hardening of steel and cast iron based automotive camshafts. *Acta Phys Pol A* 131: 374–378. https://doi.org/10.12693/APhysPolA.131.374
44. Belkin P, Kusmanov S (2016) Plasma electrolytic hardening of steels: review. *Surf Engin Appl Electrochem* 52: 531–546. https://doi.org/10.3103/S106837551606003X
45. Bayati M, Molaei R, Janghorban K (2011) Surface alloying of carbon steels from electrolytic plasma. *Met Sci Heat Treat* 53: 91–94. https://doi.org/10.1007/s11041-011-9347-5
46. Rakhadilov B, Satbayeva Z, Bayatanova L, et al. (2019) Influence of electrolyte-plasma surface hardening on the structure and properties of steel 40KhN. *J Phys Conf Ser* 1393: 012119. https://doi.org/101088/1742-6596/1393/1/012119
47. Ayday A, Durman M (2013) Surface hardening of ductile cast iron by electrolytic plasma technology. *Acta Phys Pol A* 123: 291–293. https://doi.org/10.12693/APhysPolA.123.291

48. Gorelik S (2002) *X-ray and Electron-optical Analysis*, 4 Eds., Moscow: Publishing house MISIS, 360 p (in Russian). Available from: https://www.geokniga.org/bookfiles/geokniga-rentgenograficheskiy-analiz.pdf.
49. Rastkar A, Shokri B (2012) Surface modification and wear test of carbon steel by plasma electrolytic nitrocarburizing. *Surf Interface Anal* 44: 342–351. https://doi.org/10.1002/sia.3808
50. Zhang L, Jin Y, Wang X, et al. (2019) Surface alloys of 0.45 C carbon steel produced by high current pulsed electron beam. *High Temp Mater Process* 38: 444–451. https://doi.org/10.1515/htmp-2018-0065
51. Zheng B, Huang Z, Xing J, et al. (2016) Three-body abrasive behavior of cementite–iron composite with different cementite volume fractions. *Tribol Lett* 62: 1–11. https://doi.org/10.1007/s11249-016-0683-x
52. Yaghmazadeh M, Dehghanian C (2009) Surface hardening of AISI H13 steel using pulsed plasma electrolytic carburizing (PPEC). *Plasma Processes Polym* 6: S168–S172. https://doi.org/10.1002/ppap.200930410
53. Kurbanbekov S, Skakov M, Baklanov V, et al. (2017) Changes in mechanical properties and structure of electrolytic plasma treated× 12 CrNi18 10 Ti stainless steel. *Mater Test* 59: 361–365. https://doi.org/10.3139/120.111014
54. Skakov M, Zhurerova L, Scheffler M (2013) Influence of regimes electrolytic-plasma processing on phase structure and hardening of steel 30CrMnSi. *Adv Mat Res* 601: 79–83. https://doi.org/10.4028/www.scientific.net/AMR.601.79
55. Tabieva E, Zhurerova L, Baizhan D (2020) Influence of electrolyte-plasma hardening technological parameters on the structure and properties of banding steel 2. *Key Eng Mater* 839: 57–62. https://doi.org/10.4028/www.scientific.net/KEM.839.57
56. Bayati M, Molaei R, Janghorban K (2010) Surface modification of AISI 1045 carbon steel by the electrolytic plasma process. *Metall Mater Trans A* 41: 906–911. https://doi.org/10.1007/s11661-009-0165-y
57. Nunura C, Santos C, Spim J (2015) Numerical–experimental correlation of microstructures, cooling rates and mechanical properties of AISI 1045 steel during the Jominy end-quench test. *Mater Des* 76: 230–243. https://doi.org/10.1016/j.matdes.2015.03.031
58. Li Q, Xiao K, Lu Z, et al. (2024) Mechanism of laser carbonitriding enhancing the wear resistance of 45# steel. *Mater Today Commun* 38: 108327. https://doi.org/10.1016/j.mtcomm.2024.108327
59. Korotkov V (2015) Wear resistance of carbon steel with different types of hardening. *J Frict Wear* 36: 149–152. https://doi.org/10.3103/S1068366615020105
60. Algodi S, Salman A, Al-Helli A (2023) Microstructure and mechanical properties of AISI 1106/AISI 1045 steels drawn arc stud welded joints. *Adv Sci Technol Res J* 17: 48–55. https://doi.org/10.12913/22998624/171020

AIMS Press